# Phase diffusion and fluctuations in a dissipative Bose-Josephson junction

Abhik Kumar Saha [1], Deb Shankar Ray [2,*] and Bimalendu Deb [1,†]

[1]*School of Physical Sciences, Indian Association for the Cultivation of Science, Jadavpur, Kolkata 700032, India*
[2]*School of Chemical Sciences, Indian Association for the Cultivation of Science, Jadavpur, Kolkata 700032, India*

We analyze the phase diffusion, quantum fluctuations and their spectral features of a one-dimensional Bose-Josephson junction (BJJ) nonlinearly coupled to a bosonic heat bath. The phase diffusion is considered by taking into account of random modulations of the BJJ modes causing a phase loss of initial coherence between the ground and excited states, whereby the frequency modulation is incorporated in the system-reservoir Hamiltonian by an interaction term linear in bath operators but nonlinear in system (BJJ) operators. We examine the dependence of the phase diffusion coefficient on the on-site interaction and temperature in the zero- and $\pi$-phase modes and demonstrate its phase transition-like behavior between the Josephson oscillation and the macroscopic quantum self-trapping (MQST) regimes in the $\pi$-phase mode. Based on the thermal canonical Wigner distribution, which is the equilibrium solution of the associated quantum Langevin equation for phase, coherence factor is calculated to study phase diffusion for the zero- and $\pi$-phase modes. We investigate the quantum fluctuations of the relative phase and population imbalance in terms of fluctuation spectra which capture an interesting shift in Josephson frequency induced by frequency fluctuation due to nonlinear system-reservoir coupling, as well as the on-site interaction-induced splitting in the weak dissipative regime.

## I. INTRODUCTION

A dynamical system in contact with a reservoir has been a subject of wide attention in dissipative dynamics [1,2]. Over the years, the dissipative quantum systems under the effect of random noise have been extensively investigated both theoretically and experimentally [3–7] in widely different areas, such as condensed matter physics, quantum optics, magnetic resonance spectroscopy, etc. In recent years, the study of quantum dissipation in ultracold atomic gases has attracted much attention due to the presence of various loss processes affecting the coherence of the atomic matter waves [8–10]. Also, an ultracold atomic system has become a test bed to study dissipation in an out-of-equilibrium quantum many-body system [11–16]. Apart from dephasing and relaxation dynamics, the combined effect of interaction and dissipation in open quantum systems can give rise to nonequilibrium steady states and transitions between them [17–20]. The Bose-Josephson junction (BJJ) is an ideal system where both the effects of interaction and dissipation can be explored to understand coherent and incoherent quantum dynamics of matter waves [21,22].

There are various ways in which the dissipation can be introduced in a system. The presence of an intrinsic coupling between a Josephson mode and quasiparticle excitations can lead to dissipation in a BJJ [23,24]. Dissipation also originates from the finite temperature effects [25–27] and the coupling of the system with external environment [28]. Phase fluctuation and heating effect in a BJJ due to thermal fluctuations have

been already observed in an experiment [29]. In this context, phase diffusion plays a fundamental role in the dynamical behavior of cold atoms in optical lattices and Bose-Einstein condensates (BECs) [30–40]. There are many theoretical and experimental works suggesting that the interaction between the particles can lead to phase diffusion [30–33,41–47]. Moreover, dissipation and dephasing may be engineered in an ultracold atomic system with lasers or with the assistance of a cavity [48–51]. In particular, we refer to Ref. [22,52–65] for recent investigations in theory and experiments on dissipative BJJs.

The traditional treatments of dissipation concern bilinear coupling between the system and the reservoir modes. Pure phase relaxation, however, cannot be described by such an interaction linear in both system and bath coordinates since it causes dissipation of energy and no frequency fluctuation. On the other hand, pure phase relaxations [66–70] can result from fluctuations of the energy levels of the system leading to the phase loss of initial coherence between its ground and excited states. This can be incorporated in the system-reservoir interaction by introducing a term of the form $\mathcal{F}(a, a^\dagger) \sum_j (g_j b_j + g_j^* b_j^\dagger)$, where $\mathcal{F}$ is a function of the annihilation(creation) operator $a(a^\dagger)$ for the system mode and $b_j(b_j^\dagger)$ refers to the same for $j$th reservoir mode, $g_j$ being the $j$th coupling coefficient. Such a term arises for coupling (which is linear in bath coordinates and nonlinear in system coordinates) of the type $q^2 \sum_j g_j x_j$ when expressed as $(a + a^\dagger)^2 \sum_j g_j (b_j + b_j^\dagger)$. In molecular physics $q^2 x$ is responsible for Fermi resonance [69]. A coupling of the form $H_s \sum_j (g_j b_j + g_j^* b_j^\dagger)$ where $H_s$ is the system Hamiltonian [67] may induce a coherent contribution to phase diffusion.

*pcdsr@iacs.res.in
†Corresponding author: msbd@iacs.res.in

The role of such nonlinear system-reservoir interaction in two-dimensional spectroscopy [69], thermal rectification, and differential thermal conductance [70] was studied earlier. The recent advances in bath engineering using a relatively broadband laser has opened up new directions in open quantum systems [50,51,71–77]. Guided by these considerations we examine a minimal model for system-assisted nonlinear interaction in which fluctuations of the BJJ modes become coupled to the bath coordinates. Thus the interaction induces a coherent contribution of excitation-deexcitation of the system to phase diffusion in a one-dimensional (1D) dissipative BJJ.

Based on a two-mode Hamiltonian description we derive the quantum Langevin dynamics of relative phase and population imbalance. The phase diffusion coefficient for zero- and $\pi$-phase modes reveals its characteristic dependence on the on-site interaction and temperature of the system. We find that the phase diffusion coefficient is sensitive to the variation of temperature for small dissipation. In the $\pi$-phase mode it exhibits an interesting phase transition-like behavior between the Josephson oscillation and the macroscopic quantum self-trapping (MQST) regime. Making use of the thermal canonical Wigner distribution [78], we calculate the coherence factor [79] which reveals that the 1D system-assisted dissipative BJJ has a higher degree of coherence which is consistent with the experimental observation [29]. The underlying quantum fluctuations in population imbalance and relative phase have been analyzed in terms of fluctuation spectra to demonstrate the transition between the coherent and incoherent behavior of the system from weak to strong dissipation regime and to capture the frequency-fluctuation induced shift of the Josephson frequency.

The paper is organized in the following way. In Sec. II we derive the dissipative BJJ equations by coupling the two-mode Hamiltonian to the bosonic baths in the presence of noise. In Sec. III we analyze the theoretically phase diffusion coefficient in a 1D dissipative BJJ. In Sec. IV we derive the general formula for the fluctuation spectra of population imbalance and phase difference. In Sec. V we present and discuss our results on numerical simulations of coherence factor, phase diffusion coefficient, and the spectra of the fluctuation to corroborate the theoretical scheme. The paper is concluded in Sec. VI.

## II. DISSIPATIVE BOSE-JOSEPHSON JUNCTION: A PHASE DIFFUSION MODEL

The many-body Hamiltonian for a system of $N$ bosons at zero temperature is given by

$$\hat{H}_{\mathrm{MB}} = \hat{H}_0 + \hat{H}_{\mathrm{int}}, \tag{1}$$

where

$$\hat{H}_0 = \int d\mathbf{r} \left[ -\frac{\hbar^2}{2m} \hat{\psi}^\dagger \nabla^2 \hat{\psi} + \hat{\psi}^\dagger V_{\mathrm{ext}} \hat{\psi} \right]$$

$$\hat{H}_{\mathrm{int}} = \frac{2\pi \hbar^2 a_s}{m} \int d\mathbf{r} \, \hat{\psi}^\dagger \hat{\psi}^\dagger \hat{\psi} \hat{\psi},$$

where $\hat{\psi}$ and $\hat{\psi}^\dagger$ represent bosonic fields and $V_{\mathrm{ext}}$ is the external trap potential [80,81] of the form $V_{\mathrm{ext}} = V(\rho) + V_{\mathrm{dw}}(x)$,

where $V(\rho) = \frac{1}{2} m \omega_\rho^2 \rho^2$, which permits harmonic oscillations with frequency $\omega_\rho$ along radial directions i.e., $y$- and $z$-axes and a symmetric double-well (DW) potential $V_{\mathrm{dw}}(x)$ along the $x$ axis. Here $\rho^2 = y^2 + z^2$, $a_s$ denotes the $s$-wave scattering length, and $m$ is the atomic mass. In the strong radial confinement regime ($\omega_\rho \gg \omega_x$) where $\omega_x$ be the axial frequency, we assume that all the atoms occupy the ground state of the radial harmonic potential. To proceed further, we integrate over the radial harmonic oscillator states and obtain an effective 1D Hamiltonian for the system. The lowest two energy eigenfunctions are quasidegenerate. For symmetric DW, the lowest eigenstate $\phi_g$ is space-symmetric [$\phi_g(x) = \phi_g(-x)$], and the other quasidegenerate state $\phi_e(x)$ is antisymmetric [$\phi_e(x) = -\phi_e(-x)$].

The field operator $\hat{\psi}$ can be written as

$$\hat{\psi} = \hat{a}_g \phi_g + \hat{a}_e \phi_e \tag{2}$$

with $\hat{a}_g$ and $\hat{a}_e$ ($\hat{a}_g^\dagger$ and $\hat{a}_e^\dagger$) being the annihilation (creation) operators for a particle in the ground and first excited states, respectively. The operators obey the standard bosonic commutation relation $[\hat{a}_i, \hat{a}_j^\dagger] = \delta_{ij}$. By defining further two operators $\hat{a}_L = \frac{1}{\sqrt{2}}(\hat{a}_g + \hat{a}_e)$ and $\hat{a}_R = \frac{1}{\sqrt{2}}(\hat{a}_g - \hat{a}_e)$ and their Hermitian counterparts, the effective 1D field operator becomes

$$\hat{\psi} = \hat{a}_L \phi_+ + \hat{a}_R \phi_-, \tag{3}$$

where $\phi_+ = \frac{1}{\sqrt{2}}(\phi_g + \phi_e)$ and $\phi_- = \frac{1}{\sqrt{2}}(\phi_g - \phi_e)$. The validity of this two-mode approximation for BEC rests on the fulfillment of the two conditions: (a) the temperature is much below $\hbar\omega_x$ (and so also much below $\hbar\omega_\rho$) and (b) both the interaction energy per particle and the chemical potential are much below $\hbar\omega_x$. Making use of the field operators in the many-body Hamiltonian of Eq. (1), we obtain a two-mode Hamiltonian of the form

$$\hat{H}_{\mathrm{TM}} = \hat{a}_L^\dagger \hat{a}_L E_1 + \hat{a}_R^\dagger \hat{a}_R E_2 - (\hat{a}_L^\dagger \hat{a}_R + \hat{a}_R^\dagger \hat{a}_L) K$$
$$+ \frac{U_+}{2} \hat{a}_L^\dagger \hat{a}_L^\dagger \hat{a}_L \hat{a}_L + \frac{U_-}{2} \hat{a}_R^\dagger \hat{a}_R^\dagger \hat{a}_R \hat{a}_R, \tag{4}$$

where

$$K = -\int \left[ \frac{\hbar^2}{2m} (\nabla_x \phi_+ \nabla_x \phi_-) + \phi_+ V_{\mathrm{dw}}(x) \phi_- \right] dx,$$

$$E_{1(2)} = \int \left[ \frac{\hbar^2}{2m} |\nabla_x \phi_{+(-)}|^2 + |\phi_{+(-)}|^2 V_{\mathrm{dw}}(x) \right] dx,$$

and

$$U_{+(-)} = \frac{4\pi \hbar^2 a_s}{m} \int |\phi_{+(-)}|^4 \, dx,$$

where $\nabla_x \equiv \frac{\partial}{\partial x}$, $K$ is the tunneling amplitude between two sites of the DW, and $U_{+(-)}$ is the on-site interaction strength for left(right) side of the DW arising out of nonlinearity. For a symmetric DW potential, we write $E_1 = E_2 = E$.

### A. Two-mode model coupled to bosonic heat baths

Usually Josephson oscillations in a DW potential are nondissipative, implying that the dynamics of the atom number imbalance and relative phase remains undamped over time

[82–84]. However, in recent years several studies reported a dissipative BJJ which is analogous to a pendulum with friction [85–87]. In order to study the effects of dissipation in BJJ, we consider a model of a BJJ coupled to two bosonic baths described by the total Hamiltonian

$$\hat{H}_{\mathrm{T}} = \hat{H}_{\mathrm{TM}} + \hbar \sum_{k,m=L,R} \omega_k(\hat{b}^\dagger_{\mathrm{mk}}\hat{b}_{\mathrm{mk}})$$

$$+ \hbar \sum_{k,m=L,R} g_k \hat{a}^\dagger_m \hat{a}_m(\hat{b}^\dagger_{\mathrm{mk}} + \hat{b}_{\mathrm{mk}}), \qquad (5)$$

where $\hat{b}_{mk}$ and $\hat{b}^\dagger_{mk}$ are the bosonic annihilation and creation operators, respectively, corresponding to the $k$th bath mode and $m$th well. $\omega_k$ represents the frequency of the $k$th bath mode, and $g_k$ represents the coupling between the $k$th bath mode and the on-site boson number. The bath-BJJ coupling constants for the $k$th bath mode for both wells are assumed to be the same. A key point in the present treatment is that the coupling between the system and the bath modes is nonlinear. Here the excitation in the bath modes is not accompanied by energetic deexcitation of the system as in the usual linear system-bath coupling [81]. Thus the coupling leads to fluctuations of the system energy levels, i.e., modulation in frequency resulting in phase loss of the BJJ modes [66–70]. The influence of the bath and the nonlinear coupling of the form (5) have been used earlier [28], and this gives rise to the phase diffusion of the system. The Heisenberg equations of motion for the system and the bath operators are given by the equations

$$\dot{\hat{a}}_L = -\frac{iE}{\hbar}\hat{a}_L + \frac{iK}{\hbar}\hat{a}_R - \frac{iU_+}{\hbar}\hat{a}^\dagger_L\hat{a}_L\hat{a}_L - i\sum_k g_k\hat{b}^\dagger_{Lk}(t)\hat{a}_L$$

$$- i\sum_k g_k\hat{b}_{Lk}(t)\hat{a}_L, \qquad (6)$$

$$\dot{\hat{a}}_R = -\frac{iE}{\hbar}\hat{a}_R + \frac{iK}{\hbar}\hat{a}_L - \frac{iU_-}{\hbar}\hat{a}^\dagger_R\hat{a}_R\hat{a}_R - i\sum_k g_k\hat{b}^\dagger_{Rk}(t)\hat{a}_R$$

$$- i\sum_k g_k\hat{b}_{Rk}(t)\hat{a}_R, \qquad (7)$$

$$\dot{\hat{b}}_{Lk} = -i\omega_k\hat{b}_{Lk} - ig_k\hat{a}^\dagger_L\hat{a}_L(t), \qquad (8)$$

$$\dot{\hat{b}}_{Rk} = -i\omega_k\hat{b}_{Rk} - ig_k\hat{a}^\dagger_R\hat{a}_R(t). \qquad (9)$$

After applying Born-Markov and secular approximation [88–90] and eliminating the high-frequency oscillation terms using the transformation $\hat{A}_{L,R} = \hat{a}_{L,R}e^{i\Omega(t-t_0)}$, we eliminate the bath degrees of freedom. The Heisenberg equations of motion take the following form:

$$\dot{\hat{A}}_L = \frac{iK}{\hbar}\hat{A}_R - \frac{iU_+}{\hbar}\hat{A}^\dagger_L\hat{A}_L\hat{A}_L - \frac{\gamma}{2}\hat{A}^\dagger_L\hat{A}_L\hat{A}_L + \hat{F}_L(t)\hat{a}_L, \quad (10)$$

$$\dot{\hat{A}}_R = \frac{iK}{\hbar}\hat{A}_L - \frac{iU_-}{\hbar}\hat{A}^\dagger_R\hat{A}_R\hat{A}_R - \frac{\gamma}{2}\hat{A}^\dagger_R\hat{A}_R\hat{A}_R + \hat{F}_R(t)\hat{a}_R, \quad (11)$$

where

$$\hat{F}_L(t) = -i\sum_k g_k(t_0)\hat{b}_{Lk}(t_0)e^{-i(\omega_k-\Omega)(t-t_0)}, \qquad (12)$$

$$\hat{F}_R(t) = -i\sum_k g_k(t_0)\hat{b}_{Rk}(t_0)e^{-i(\omega_k-\Omega)(t-t_0)} \qquad (13)$$

refer to the quantum noise due to the heat baths modulated by oscillation of the system for the $L$ and $R$ modes. $\gamma$ represents the dissipation of the system modes and $\Omega = E/\hbar$. Equations (10) and (11) and the noise operators in Eqs. (12) and (13) appear as a natural consequence of system-reservoir couplings. The detailed derivation of Eqs. (10) and (11) is presented in Appendix A.

To construct a quantum Langevin equation with $c$-number noise [91,92], we return to Eqs. (10) and (11) and carry out a quantum mechanical average over the initial product separable quantum states of the system oscillator and the bath oscillators at $t_0 = 0$ $|\alpha\rangle|\mu_1\rangle|\mu_2\rangle\cdots|\mu_k\rangle\cdots|\mu_N\rangle$. Here $|\alpha\rangle$ refers to the initial coherent state of the system, and $\{|\mu_k\rangle\}$ corresponds to the initial coherent states of the bath operators. We denote the quantum mechanical averages for the system and the bath operators as $\langle\hat{A}_{L,R}\rangle = \alpha_{L,R}$, $\langle\hat{A}^\dagger_{L,R}\rangle = \alpha^*_{L,R}$, and $\langle\hat{F}_{L,R}\rangle = \xi_{L,R}$. Here $\xi_{L,R} = -i\sum_k g_k(t_0)\mu_{Lk,Rk}e^{-i(\omega_k-\Omega)(t-t_0)}$. The $c$-number noise with zero mean follows the fluctuation-dissipation relation, such that $\langle\xi_{L,R}(t)\rangle = 0$ and $\langle\xi^*_{L,R}(t)\xi_{L,R}(t')\rangle = \gamma\coth(\hbar\Omega/2k_BT)\delta(t-t')$. The thermal properties of quantum noise are presented in detail in Appendix B. The $c$-number amplitudes may now be written as $\alpha_L = \sqrt{N_L}e^{i\theta_L}$ and $\alpha_R = \sqrt{N_R}e^{i\theta_R}$. $N_{L(R)}$ is the number of atoms in the left (right) well. $\theta_{L(R)}$ is the phase of the atoms in the left (right) well. The complex amplitude equations for two wells are given by

$$\dot{\alpha}_L = \frac{iK}{\hbar}\alpha_R - \frac{iU_+}{\hbar}N_L\alpha_L - \frac{\gamma}{2}N_L\alpha_L + \xi_L(t)\alpha_L, \quad (14)$$

$$\dot{\alpha}_R = \frac{iK}{\hbar}\alpha_L - \frac{iU_-}{\hbar}N_R\alpha_R - \frac{\gamma}{2}N_R\alpha_R + \xi_R(t)\alpha_R. \quad (15)$$

In deriving the above equations, the mean-field approximation is used whereby the coherent state average over the terms like $\hat{A}^\dagger_L\hat{A}_L\hat{A}_L$ is replaced by $\langle\hat{A}^\dagger_L\hat{A}_L\rangle\langle\hat{A}_L\rangle$ or $N_L\alpha_L$, i.e., we have taken into account the quantum correlations in the lowest order. The underlying assumption is that the fluctuation around the mean is small. In terms of the Ginzburg criterion this implies $\langle\delta\hat{A}^\dagger_L\delta\hat{A}_L\rangle \ll \langle\hat{A}^\dagger_L\hat{A}_L\rangle$, which is reasonably good when the number of atoms in the condensate is not too low.

Separating the real and imaginary parts of Eqs. (14) and (15) we obtain after some algebra the following equations in terms of the normalized atom number imbalance $z(t)$ and phase difference $\theta(t)$:

$$\dot{z}(t) = -\frac{2K}{\hbar}\sqrt{1-z^2(t)}\sin\theta(t) - \gamma Nz(t) + \xi_z, \quad (16)$$

$$\dot{\theta}(t) = \frac{2K}{\hbar}\left[\frac{z(t)}{\sqrt{1-z^2(t)}}\cos\theta(t) + \Lambda_0 z(t)\right] + \xi_\theta, \quad (17)$$

where $\xi_z = 2\xi_L(t)N_L/N - 2\xi_R(t)N_R/N$, $\xi_\theta = \xi_R - \xi_L$, and $z = \frac{|\alpha_L|^2 - |\alpha_R|^2}{|\alpha_L|^2 + |\alpha_R|^2} = \frac{N_L - N_R}{N_L + N_R}$. The conjugate variable is the relative phase defined by $\theta = \theta_R - \theta_L$. $\Lambda_0(= \frac{NU}{2K})$ characterizes the many-body interaction parameter with $U$ being the on-site mean two-body interaction energy where $U = \frac{U_+ + U_-}{2}$. Now for symmetric DW, we consider $U_+ = U_- = U$. Equations (16) and (17) represent the dissipative BJJ equation with noise. The detailed derivation of Eqs. (16) and (17) is presented in Appendix C. In the absence of noise [$\xi_{L,R}(t) = 0$] the equations reduce to the dissipative BJJ equations in

which the dissipative coefficient term can be modified by the linear contribution from $\dot{\theta}(t)$, which is usually studied in the standard dissipative BJJ [81,85,86,93]. In the absence of dissipation ($\gamma = 0$) Eqs. (16) and (17) reduce to the standard BJJ equations.

## III. PHASE DRIFT AND DIFFUSION

Equations (16) and (17) describe the BJJ equations with quantum noise. These are nonlinear Langevin equations which cannot be solved by any direct analytical method. The traditional way to circumvent this difficulty is to resort to the

weak noise limit. To this end we consider first the steady state of the system in the absence of noise and linearize the dynamics around it. We are then led to a multivariate Ornstein-Uhlenbeck (OU) process as considered below.

To proceed, we begin with the steady states of the dynamical system $(z_s, \theta_s)$. These steady states are the zero-phase mode ($z_s = 0$, $\theta_s = 0$), $\pi$-phase mode ($z_s = 0$, $\theta_s = \pi$), and $\pi$-phase self-trapping mode ($z_s = \pm\sqrt{1 - \frac{1}{\Lambda_0^2}}$, $\theta_s = \pi$). Now linearizing the system around $(z_s, \theta_s)$ with $z = z_s + \delta z$ and $\theta = \theta_s + \delta\theta$, where $\delta z$ and $\delta\theta$ are small perturbations, we obtain the linearized Langevin equations in $c$-numbers

$$\delta\dot{z} = -\frac{2K}{\hbar}\sqrt{1 - z_s^2}\cos\theta_s\,\delta\theta + \frac{2K}{\hbar}\frac{z_s\delta z}{\sqrt{1 - z_s^2}}\sin\theta_s - \gamma N\delta z + \xi_z(t), \tag{18}$$

$$\delta\dot{\theta} = \frac{2K}{\hbar}\left[\Lambda_0\delta z - \frac{z_s\sin\theta_s}{\sqrt{1 - z_s^2}}\delta\theta + \frac{\cos\theta_s}{(1 - z_s^2)^{\frac{3}{2}}}\delta z\right] + \xi_\theta(t), \tag{19}$$

where $\xi_z(t) = \xi_L(t) - \xi_R(t) + z_s[\xi_L(t) + \xi_R(t)]$ and $\xi_\theta(t) = \xi_R(t) - \xi_L(t)$. Here we have used the relations $N_{Ls,Rs} = \frac{N}{2}(1 \pm z_s)$. $N_{Ls,Rs}$ are the steady-state values of the number of atoms in the left and right wells. For $\gamma > 0$, $\delta z$ gets equilibrated at a fast rate. One can therefore resort to adiabatic elimination of the fast variable $z$, which results in

$$\delta z = \frac{\frac{2K}{\hbar}\sqrt{1 - z_s^2}\cos\theta_s\,\delta\theta - \xi_z}{\frac{2K}{\hbar}\frac{z_s\sin\theta_s}{\sqrt{1 - z_s^2}} - \gamma N}.$$

Now inserting $\delta z$ in Eq. (19), we obtain after some algebra an equation in the form of linear Langevin dynamics for phase $\delta\theta(t)$:

$$\delta\dot{\theta} = -\eta\delta\theta + C\xi_z(t) + \xi_\theta(t), \tag{20}$$

where $\eta$ is the linear phase drift. The general expressions for $\eta$ and $C$ are

$$\eta = \frac{2K}{\hbar}\left[\frac{z_s\sin\theta_s}{\sqrt{1 - z_s^2}} - \frac{\cos\theta_s}{(1 - z_s^2)^{\frac{3}{2}}}\left(\frac{\sqrt{1 - z_s^2}\cos\theta_s}{\frac{z_s\sin\theta_s}{\sqrt{1 - z_s^2}} - \frac{\gamma N\hbar}{2K}}\right) - \Lambda_0\left(\frac{\sqrt{1 - z_s^2}\cos\theta_s}{\frac{z_s\sin\theta_s}{\sqrt{1 - z_s^2}} - \frac{\gamma N\hbar}{2K}}\right)\right] \tag{21}$$

and

$$C = -\frac{\cos\theta_s}{(1 - z_s^2)^{\frac{3}{2}}}\left(\frac{1}{\frac{z_s\sin\theta_s}{\sqrt{1 - z_s^2}} - \frac{\gamma N\hbar}{2K}}\right) - \Lambda_0\left(\frac{1}{\frac{z_s\sin\theta_s}{\sqrt{1 - z_s^2}} - \frac{\gamma N\hbar}{2K}}\right), \tag{22}$$

respectively. It is important to emphasize that as $\delta z$ saturates, $\delta\theta$ is governed by diffusion and drift. The drift $\eta$ [Eq. (21)] contains $\gamma$. A closer look at the steady states $(z_s, \theta_s)$ and their substitution in expression (21) indicates that $\eta$ is always positive. Thus $\delta\theta$ cannot grow indefinitely but is governed by Brownian dynamics following the fluctuation-dissipation relation, so that $\delta\theta$ equilibrates in time.

Making use of the fluctuation-dissipation relation for $c$-number noise with zero mean [Eqs. (B6) and (B7)] it follows

$$\langle\xi(t)\xi(t')\rangle = C^2(1 + z_s^2)2\gamma\coth(\hbar\Omega/2k_BT)\delta(t - t'),$$

where $\xi(t) = C\xi_z(t) + \xi_\theta(t)$. The Fokker-Planck equation corresponding to the linear Langevin dynamics [Eq. (20)] is given by [89]

$$\frac{\partial P(\Psi, t)}{\partial t} = -\frac{\partial}{\partial\Psi}(\eta\Psi)P(\Psi, t) + \mathcal{D}\frac{\partial^2 P(\Psi, t)}{\partial\Psi^2}. \tag{23}$$

Here $P(\Psi, t)$ is the probability of finding $\Psi$ at time $t$; we have put $\delta\theta \equiv \Psi$. $\mathcal{D}$ is the phase diffusion coefficient as given by

$$\mathcal{D} = C^2\gamma(1 + z_s^2)\coth(\hbar\Omega/2k_BT). \tag{24}$$

A clear separation of the statistical part $\coth(\hbar\Omega/2k_BT)$ from the dynamical prefactor is quite apparent in the above expression. The expression for phase diffusion coefficient is one of the main results of this section. Equation (23) shows that phase perturbation can be described as Brownian motion of a particle characterized by phase drift and diffusion. At finite temperature, the macroscopic quantum tunneling across 1D dissipative BJJ is thus significantly affected by number and phase fluctuations.

Before closing this section, we digress a little bit about the consistency check of the calculation. Putting the Fokker-Planck equation (23) in the form of a continuity equation $\frac{\partial P}{\partial t} + \frac{\partial F}{\partial\Psi} = 0$, we identify the flux [89]

$$F = -\left(\eta\Psi P + \mathcal{D}\frac{\partial P}{\partial\Psi}\right).$$

At equilibrium $F = 0$, we obtain from the above equation the equilibrium distribution function

$$P_{\text{equ}}(\Psi) = A \exp\left[-\left(\frac{\kappa^{-1}}{2\coth\left(\frac{\hbar\Omega}{2k_BT}\right)}\right)\Psi^2\right] \quad (25)$$

for the zero-phase mode $\kappa = \frac{1+\Lambda_0}{N}$, $\pi$-phase mode $\kappa = \frac{1-\Lambda_0}{N}$, and $\pi$-phase self-trapping mode $\kappa = \frac{\Lambda_0^2(\Lambda_0^2-1)}{N}$. $T$ is the temperature and $A$ is the normalization constant, respectively. The distribution does not depend on $\gamma$ as it should for the attainment of equilibrium. Second, the width is governed by the coth function, which carries the signature of Wigner canonical thermal distribution (B4) employed in the course of construction of the ensemble for $c$-number noise in the present treatment. Third, the occurrence of the $\Psi^2$ term in the parentheses of the distribution is reminiscent of the potential energy term of an equilibrium distribution.

## IV. SPECTRUM OF FLUCTUATIONS

We now go beyond the adiabatic elimination of a fast variable to calculate the spectra of the fluctuation of number imbalance and phase difference associated with the BJJ dynamics. To proceed we recast Eqs. (18) and (19) in matrix form as

$$\dot{\beta}(t) = -B\beta(t) + M(t), \quad (26)$$

where

$$\beta = \begin{pmatrix} \delta z \\ \delta\theta \end{pmatrix}, \quad B = \begin{pmatrix} \gamma N - \frac{2K}{\hbar}\frac{z_s\sin\theta_s}{\sqrt{1-z_s^2}} & \frac{2K}{\hbar}\sqrt{1-z_s^2}\cos\theta_s \\ -\frac{2K}{\hbar}\left(\Lambda_0 + \frac{\cos\theta_s}{(1-z_s^2)^{\frac{3}{2}}}\right) & \frac{2K}{\hbar}\frac{z_s\sin\theta_s}{\sqrt{1-z_s^2}} \end{pmatrix}, \quad M = \begin{pmatrix} \xi_z \\ \xi_\theta \end{pmatrix}$$

such that $\beta\beta^T \equiv \beta \times \beta$ is a direct product of the matrix

$$\beta \times \beta = \begin{pmatrix} \delta z(t)\delta z(t) & \delta z(t)\delta\theta(t) \\ \delta\theta(t)\delta z(t) & \delta\theta(t)\delta\theta(t) \end{pmatrix}.$$

Taking the average on both sides of Eq. (26) we obtain

$$\langle\dot{\beta}(t)\rangle = -B\langle\beta(t)\rangle + \langle M(t)\rangle.$$

By virtue of the zero mean of $c$-number noise $\langle\xi_{L,R}(t)\rangle = 0$, we have $\langle M(t)\rangle = 0$. Direct integration yields

$$\langle\beta(t)\rangle = e^{-Bt}\langle\beta(0)\rangle,$$

where $\langle\beta(0)\rangle$ gives the average of the initial value $\langle\beta(t)\rangle$. Now, according to the regression theorem the correlation function decays in the same way as the average decay, which suggests that

$$\langle\beta(t)\beta(0)\rangle = e^{-Bt}\langle\beta(0)\beta(0)\rangle,$$

$$\langle\beta(0)\beta(t)\rangle = \langle\beta(0)\beta(0)\rangle e^{-B^Tt}. \quad (27)$$

To obtain the low-frequency spectrum of various modes of correlation, we calculate the Fourier transform of $\langle\beta(t)\beta(0)\rangle$ and define

$$\mathcal{S}(\Delta) = \int_{-\infty}^{+\infty} e^{-i\Delta It}\langle\beta(t)\beta(0)\rangle\,dt, \quad (28)$$

where $\Delta$ refers to the detuning around $\Omega$, $I$ is the identity matrix and $t = 0$ refers to the stationary state, i.e., we calculate the correlation of fluctuation around the stationary state. On further manipulation of Eqs. (28) and (27), we obtain

$$\mathcal{S}(\Delta) = (B + i\Delta I)^{-1}\langle\beta(0)\beta(0)\rangle + \langle\beta(0)\beta(0)\rangle(B^T - i\Delta I)^{-1}.$$

The stationary state contribution in the above equation can be expressed in terms of the diffusion matrix of the form

$$\mathcal{D}_{z,\theta} = \begin{pmatrix} \gamma\left(1 + z_s^2\right)\coth(\hbar\Omega/2k_BT) & 0 \\ 0 & \gamma\coth(\hbar\Omega/2k_BT) \end{pmatrix}$$

so that the $2 \times 2$ fluctuation spectrum matrix becomes

$$\mathcal{S}(\Delta) = (B + i\Delta I)^{-1}2\mathcal{D}_{z,\theta}(B^T - i\Delta I)^{-1}.$$

Explicit evaluation of the matrix elements results in the fluctuations of number imbalance as the $\mathcal{S}_{11}$ element, while the $\mathcal{S}_{22}$ element represents the contribution due to phase fluctuation [88].

The number fluctuation spectrum ($\mathcal{S}_{11}$ element) can be written as

$$\mathcal{S}_z(\Delta) = \frac{2\mathcal{D}_{11}\left(B_{22}^2 + \Delta^2\right) + 2\mathcal{D}_{22}B_{12}^2}{(B_{11}B_{22} - B_{12}B_{21} - \Delta^2)^2 + \Delta^2(B_{11} + B_{22})^2}. \quad (29)$$

Similarly, the phase fluctuation term ($\mathcal{S}_{22}$ element) can be written as

$$\mathcal{S}_\theta(\Delta) = \frac{2\mathcal{D}_{11}B_{21}^2 + 2\mathcal{D}_{22}\left(B_{11}^2 + \Delta^2\right)}{(B_{11}B_{22} - B_{12}B_{21} - \Delta^2)^2 + \Delta^2(B_{11} + B_{22})^2}, \quad (30)$$

where $B_{11} = \gamma N - \frac{2K}{\hbar}\frac{z_s\sin\theta_s}{\sqrt{1-z_s^2}}$, $B_{12} = \frac{2K}{\hbar}\sqrt{1-z_s^2}\cos\theta_s$, $B_{21} = -\frac{2K}{\hbar}\left(\Lambda_0 + \frac{\cos\theta_s}{(1-z_s^2)^{\frac{3}{2}}}\right)$, and $B_{22} = \frac{2K}{\hbar}\frac{z_s\sin\theta_s}{\sqrt{1-z_s^2}}$. The diffusion matrix elements are defined as $\mathcal{D}_{11} = \gamma(1 + z_s^2)\coth(\hbar\Omega/2k_BT)$ and $\mathcal{D}_{22} = \gamma\coth(\hbar\Omega/2k_BT)$.

## V. RESULTS AND DISCUSSION

We now discuss three distinct aspects of the present work highlighting the coherence factor, phase diffusion coefficient, and fluctuation spectra for zero- and $\pi$-phase modes. The conspicuous role of the on-site interaction and tunneling and their interplay with the system-bath coupling in controlling coherence, phase transition, and quantum fluctuation of number and phase are illustrated.

### A. Coherence factor

In order to study the coherent and incoherent regimes of the dissipative BJJ, we now define $\langle\cos\Psi\rangle$ as a coherence factor [79] as it provides the degree of coherence of the system.
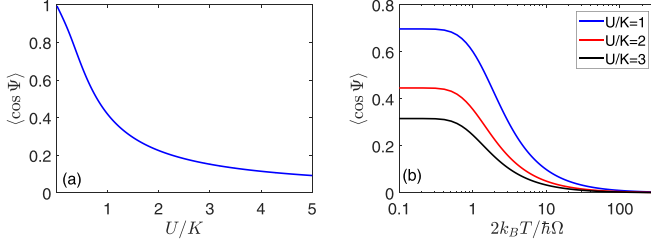
FIG. 1. (a) Variation of the coherence factor $\langle \cos \Psi \rangle$ as a function of $U/K$ at $k_B T/\hbar\Omega = 1/10$ in zero-phase mode. (b) Variation of $\langle \cos \Psi \rangle$ as a function of $2k_B T/\hbar\Omega$ for $U/K = 1$ (blue solid line), $U/K = 2$ (red solid line), and $U/K = 3$ (black solid line). Note the logarithmic scale on the horizontal axis.

If the value of the linearized phase is localized around zero, the value of the coherence factor is close to unity. If instead the phase is fully delocalized and all its values are equally probable, then the value of the coherence factor is close to zero implying that the system is in the incoherent state. Since at equilibrium the relative phase follows the Wigner thermal canonical distribution [78] as described by Eq. (25), one may define explicitly the coherence factor as follows:

$$\langle \cos \Psi \rangle = \frac{\int_{-\pi}^{\pi} d\Psi \cos \Psi \exp\left[\frac{\cos \Psi}{\kappa \coth\left(\frac{\hbar\Omega}{2k_B T}\right)}\right]}{\int_{-\pi}^{\pi} d\Psi \exp\left[\frac{\cos \Psi}{\kappa \coth\left(\frac{\hbar\Omega}{2k_B T}\right)}\right]}. \qquad (31)$$

The appearance of the factor $\kappa$ in the canonical distribution makes the coherence factor dependent on the on-site mean two-body interaction energy $U$ and the tunneling energy $K$. In what follows we examine the coherence factor in the light of these parameters.

### *1. Zero-phase mode*

For our numerical calculation in zero-phase mode, we set the total number of atoms $N = 1000$. In Fig. 1(a) we show the coherence factor $\langle \cos \Psi \rangle$ as a function of the ratio $U/K$ for the low-temperature limit $k_B T/\hbar\Omega = 1/10$ in the zero-phase mode for which $\kappa = \frac{1+\Lambda_0}{N}$. It is apparent that in the limit of strong tunneling $U/K \ll 1$, the coherence factor gets close to unity. This is because under this condition the system undergoes a small oscillation around the equilibrium zero-phase value. In this limit the fluctuation of the phase difference is also small. In the opposite limit, when $U/K \gg 1$, the amplitude of the oscillation around the equilibrium increases as a result of delocalization of the phase due to the large on-site interaction. As the phase fluctuations are not small, the coherence factor gradually decreases. This is similar to the prediction of the coherence factor calculated using the Josephson Hamiltonian [79]. In Fig. 1(b) we plot the temperature dependence of the coherence factor. It is clear that for a particular value of the interaction energy, the coherence factor at low temperature is almost constant and then with increase of temperature the coherence factor decreases. At high temperature ($2k_B T/\hbar\Omega \approx 100$), the curves coincide for different interaction energies close to zero, i.e., the system becomes incoherent. This general behavior of the coherence factor is observed over three orders of magnitude of $2k_B T/\hbar\Omega$
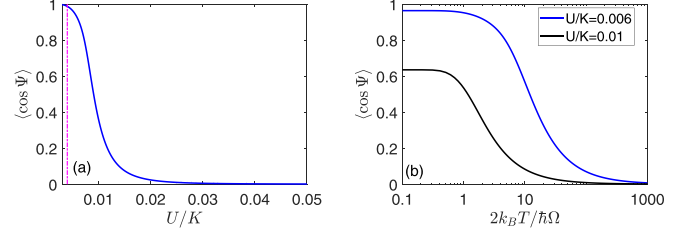
FIG. 2. (a) Variation of $\langle \cos \Psi \rangle$ as a function of $U/K$ at $k_B T/\hbar\Omega = 1/10$ in the $\pi$-phase self-trapping regime. The vertical dashed-dotted magenta line corresponds to $U/K = 0.004$. (b) Variation of $\langle \cos \Psi \rangle$ as a function of $2k_B T/\hbar\Omega$ for $U/K = 0.006$ (blue solid line) and $U/K = 0.01$ (black solid line). Note the logarithmic scale on the horizontal axis.

and is in good agreement with the experimental observation [29].

### *2. $\pi$-phase self-trapping mode*

In Fig. 2(a) we plot the coherence factor $\langle \cos \Psi \rangle$ as a function of the ratio $U/K$ for the low-temperature limit $k_B T/\hbar\Omega = 1/10$ in the $\pi$-phase self-trapping regime. In this regime $\kappa$ is given by $\kappa = \frac{\Lambda_0^2[\Lambda_0^2 - 1]}{N}$ with $\Lambda_0 > 1$. The coherence factor quickly falls from unity to zero with small change in the $U/K$ ratio. When $U/K < 0.004$, the value of the coherence factor is close to unity. In this regime the system oscillates around a nonzero value of the population imbalance and phase difference, and the fluctuation in phase remains low. When $U/K > 0.004$ the coherence factor falls off rapidly from unity to zero. In Fig. 2(a) the vertical dashed-dotted magenta line corresponds to $U/K = 0.004$, which basically separates out the $\pi$-phase self-trapping regime from the running $\pi$-phase self-trapping regime [82]. In the running $\pi$-phase self-trapping regime the population imbalance oscillates around a nonzero mean value, but the phase difference between the two BECs in the left and right wells evolves unbound as a result of which the relative phase increases monotonically. So the phase is delocalized and the phase fluctuations are not small. The system becomes incoherent. Furthermore when $U/K > 0.025$, the value of the coherence factor is almost zero signifying the incoherent regime. In Fig. 2(b) we show the temperature dependence of the coherence factor for fixed interaction energies by choosing $U/K$ in the nearly coherent regime where the system is in the running phase self-trapping mode. We observe similar behavior when compared to the case of the zero-phase mode. However, compared to the zero-phase mode the degree of coherence increases by one order of magnitude. This study of coherence reveals that the 1D dissipative BJJ has a higher degree of coherence.

### B. Phase diffusion coefficient

In this section we present our results for the variation of the phase diffusion coefficient with temperature and its phase transition-like behavior in $\pi$-phase modes.

### *1. Variation of $\mathcal{D}$ with temperature*

The dependence of the phase diffusion coefficient $\mathcal{D}$ on the interaction parameter, dissipation constant, and temperature is
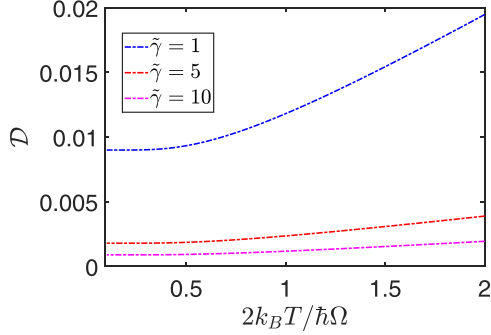
FIG. 3. Variation of the phase diffusion coefficient $\mathcal{D}$ as a function of $2k_B T/\hbar\Omega$ for different values of $\tilde{\gamma}$ with many-body interaction parameter $\Lambda_0 = 0.5$ in the zero-phase mode.



FIG. 4. Variation of $\mathcal{D}$ as a function of $\Lambda_0$ at $k_B T/\hbar\Omega = 1/10$ with $\tilde{\gamma} = 1$ in the $\pi$-phase mode. Magenta solid line depicts $\mathcal{D}$ vs $\Lambda_0$ curve for $z_s = 0, \theta_s = \pi$ and for $z_s = \pm\sqrt{1 - \frac{1}{\Lambda_0^2}}, \theta_s = \pi$; the $\mathcal{D}$ vs $\Lambda_0$ curve is depicted by solid blue and red dashed lines. The vertical black dashed line corresponds to the critical $\Lambda_0$ for the transition between Josephson oscillation and MQST in the $\pi$-phase mode. Inset: Variation of the steady-state population imbalance $z_s$ as a function of $\Lambda_0$. The three different colors signify three different steady states of the population imbalance. The vertical black dashed line corresponds to $\Lambda_0$ where the bifurcation of $z_s$ occurs.

clearly illustrated by expression (24). A representative variation of $\mathcal{D}$ as a function of temperature is shown in Fig. 3 for the zero-phase mode for several values of $\tilde{\gamma}$ for $N = 1000$. We set $U/K = 0.001$ such that the many-body interaction parameter becomes $\Lambda_0 = 0.5$ (weak interaction or the strong tunneling regime). It is observed that $\mathcal{D}$ remains constant up to $2k_B T/\hbar\Omega \approx 0.4$. On further increase of the temperature, i.e., $(2k_B T/\hbar\Omega > 0.4)$ $\mathcal{D}$ increases but for lower values of $\tilde{\gamma}$ as shown by the blue dashed-dotted line in Fig. 3. The variation is insensitive to the temperature for larger values of dissipation coefficient as evident from the magenta and red dashed-dotted lines in Fig. 3. The trend is qualitatively similar to the corresponding cases for the $\pi$-phase modes.

### *2. Variation of $\mathcal{D}$ with $\Lambda_0$*

In the $\pi$-phase mode, there are three steady-state solutions (a) $z_s = 0, \theta_s = \pi$, (b) $z_s = \sqrt{1 - \frac{1}{\Lambda_0^2}}, \theta_s = \pi$, and (c) $z_s = -\sqrt{1 - \frac{1}{\Lambda_0^2}}, \theta_s = \pi$. The first solution arises for $\Lambda_0 < 1$; the second and third solutions are acceptable for when $\Lambda_0 > 1$. At $\Lambda_0 = 1$ a bifurcation of population imbalance occurs which is plotted in the inset of Fig. 4. This bifurcation in the $\pi$-phase mode has been observed experimentally in internal BJJs [94]. To analyze the effect of this bifurcation on the phase diffusion coefficient, we plot $\mathcal{D}$ as a function of the interaction parameter $\Lambda_0$ in Fig. 4. We see that for $\Lambda_0 < 1$, i.e., when $z_s = 0, \theta_s = \pi$, the phase diffusion coefficient $\mathcal{D} \propto C^2 \gamma$ where $C = \frac{2K}{\hbar\tilde{\gamma}}[\Lambda_0 - 1]$. With an increase of $\Lambda_0$, the phase diffusion coefficient $\mathcal{D}$ decreases as represented by the solid magenta line. At $\Lambda_0 = 1$, the phase diffusion coefficient becomes zero. For $\Lambda_0 > 1$, there are two possible solutions of $z_s$, and for both cases $C$ is given by $C = \frac{2K}{\hbar\tilde{\gamma}}[\Lambda_0 - \frac{1}{\Lambda_0^3}]$. For this, we observe that $\mathcal{D}$ increases sharply with the increase of $\Lambda_0$ as represented by the blue solid and red dashed lines. $\Lambda_0 = 1$ is therefore the critical point at which a turnover of the phase diffusion coefficient occurs due to bifurcation of $z_s$. The phase transition-like behavior here originates from the symmetry breaking in BJJ in the $\pi$-phase modes. It is interesting to note that the two branches of the bifurcation in $z_s$ shown for the steady-state population imbalance (inset) coalesce on a single line for the phase diffusion coefficient in the regime $\Lambda_0 > 1$. This can be understood from the expression for phase diffusion coefficient $\mathcal{D}$, which is a function of $z_s^2$ rather than $z_s$.
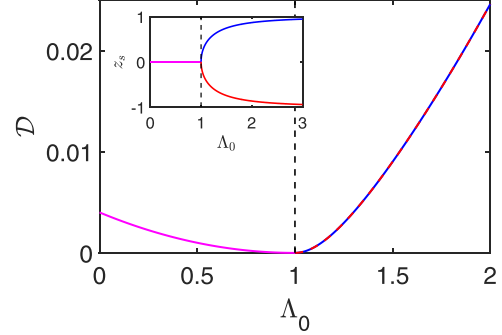
The turnover or phase transition-like behavior of $\mathcal{D}$ can be explained as follows: For a small dissipation coefficient ($\tilde{\gamma} = 1$) at low temperature ($k_B T/\hbar\Omega = 1/10$), it follows that the dynamics of the dissipative BJJ is governed by the Josephson Hamiltonian [82], which gives negative energy for the zero-phase mode and positive energy for the $\pi$-phase mode. Now, in the $\pi$-phase mode, the system initially has large energy so that the increase of $\Lambda_0$ does not change the flow of the relative phase between two wells in the DW potential as a result of which $\mathcal{D}$ decreases. At the critical $\Lambda_0$, the interaction energy, however, becomes equal to the steady-state Josephson Hamiltonian energy, which implies that at this point there is no flow of the relative phase between the wells. Further increase of $\Lambda_0$ implies that many-body interaction energy becomes large compared to the Josephson Hamiltonian energy so that the flow is reversed and as a result $\mathcal{D}$ increases. This is also similar to the case of the zero-phase mode because for this case the initial Josephson Hamiltonian energy is negative and with increase of $\Lambda_0$, $\mathcal{D}$ increases. For the sake of brevity the behavior of $\mathcal{D}$ as a function of $\Lambda_0$ in the zero-phase mode is not shown. However, it is clear that as $[\mathcal{D} \propto (1 + \Lambda_0)^2]$ $\mathcal{D}$ increases with increase of $\Lambda_0$.

### C. Quantum fluctuation spectra

From Eqs. (29) and (30), the analytical expressions for the spectra of number and phase fluctuations become

$$S_z(\Delta) = \frac{\frac{2\tilde{\gamma}}{N} \coth\left(\frac{\hbar\Omega}{2k_B T}\right)(4 + \Delta^2)}{\left(\Delta^2 - f^2 + \frac{\tilde{\gamma}^2}{2}\right)^2 + \left(f^2\tilde{\gamma}^2 - \frac{\tilde{\gamma}^4}{4}\right)},$$

$$S_\theta(\Delta) = \frac{\frac{2\tilde{\gamma}}{N} \coth\left(\frac{\hbar\Omega}{2k_B T}\right)[f^2(1 + \Lambda_0) + \tilde{\gamma}^2 + \Delta^2]}{\left(\Delta^2 - f^2 + \frac{\tilde{\gamma}^2}{2}\right)^2 + \left(f^2\tilde{\gamma}^2 - \frac{\tilde{\gamma}^4}{4}\right)},$$

respectively. Here $\tilde{\gamma} = \gamma N$ and the oscillation frequency $f = \frac{2K}{\hbar}\sqrt{1 + \Lambda_0}$ (zero-phase mode Josephson frequency),
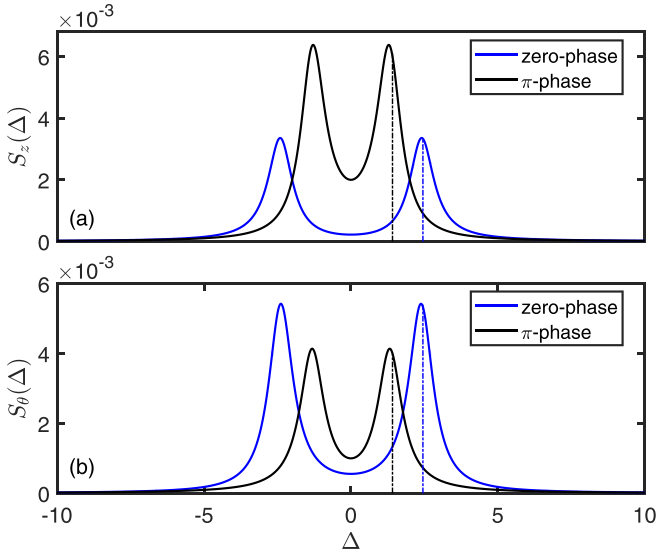
FIG. 5. Variations of the number fluctuation spectrum $\mathcal{S}_z(\Delta)$ (a) and phase fluctuation spectrum $\mathcal{S}_\theta(\Delta)$ (b) as a function of $\Delta$ for zero-phase (solid blue line) and $\pi$-phase mode (solid black line) for $U/K = 0.001$, $\tilde{\gamma} = 1$ with $N = 1000$, and $k_B T/\hbar\Omega = 1/10$. The blue and black dashed-dotted lines indicate the Josephson frequency in the absence of dissipation for zero and $\pi$-phase mode, respectively.



FIG. 6. Variations of $\mathcal{S}_z(\Delta)$ (a) and $\mathcal{S}_\theta(\Delta)$ (b) as a function of $\Delta$ for different values of $\tilde{\gamma}$ in zero-phase mode for $U/K = 0.001$, with $N = 1000$ and $k_B T/\hbar\Omega = 1/10$. The green dashed-dotted line indicates the Josephson frequency in zero-phase mode in the absence of dissipation.

$f = \frac{2K}{\hbar}\sqrt{1 - \Lambda_0}$ ($\pi$-phase mode Josephson frequency), and $f = \frac{2K}{\hbar}\sqrt{\Lambda_0^2 - 1}$ ($\pi$-phase self-trapping frequency) of the three modes.

From the above expressions we first note that when the detuning $\Delta = 0$, both number and phase fluctuations persist ($\mathcal{S}_z, \mathcal{S}_\theta \neq 0$) in zero- and $\pi$-phase modes of 1D dissipative BJJ down to absolute zero. Second, it is clear that the peak position depends on a $\tilde{\gamma}$-dependent shift from the Josephson frequency for zero- and $\pi$-phase modes and the self-trapping frequency for the respective mode. We emphasize that this frequency shift is a direct consequence of the nonlinear system-bath interaction in which the fluctuation in energy levels of the system causes a phase loss of initial coherence without dissipation. Third, depending on the relative strength of $\tilde{\gamma}$, i.e., the system-reservoir coupling and the on-site interaction $\Lambda_0$, the phase and number fluctuation spectra may exhibit a single- or double-peak structure. The interaction ($\Lambda_0$)-induced splitting when $\tilde{\gamma}$ is small is reminiscent of the Autler-Townes doublet in quantum optics. We now illustrate the main results for the fluctuation spectra.

We first examine the general spectral characteristics in the weak on-site interaction and weak dissipation regime in the zero- and $\pi$-phase mode. For this we set $k_B T/\hbar\Omega = 1/10$, $U/K = 0.001$, and $\tilde{\gamma} = 1$ with total number of atoms $N = 1000$. In Figs. 5(a) and 5(b), we plot the number and phase fluctuation spectra as a function of detuning for the zero-phase mode denoted by the solid blue line and for the $\pi$-phase Josephson oscillation regime indicated by the solid black line. For each mode, we observe that two peaks appear where the dashed-dotted lines indicate the Josephson frequency in the respective modes. It is clear that exactly at the shifted Josephson frequency the amplitude of the number and phase fluctuation spectra is maximum. In the $\pi$-phase mode the am-
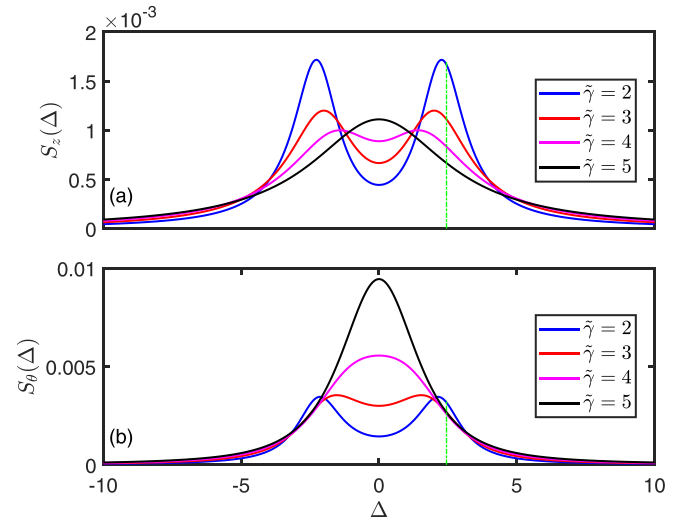
plitude of the number fluctuation spectrum is higher compared to that in the zero-phase mode for the same $\Delta$ value, and the opposite behavior is observed for the phase fluctuation spectra. We also observe that the difference between the maximum and minimum of the spectra at $\Delta = 0$ is large for the $\pi$-phase mode number fluctuation spectra compared to that for the corresponding zero-phase mode. The reason behind this behavior is that for a fixed many-body interaction parameter the Josephson frequency for the zero-phase mode is always greater than that for the $\pi$-phase mode. As a result when the Josephson frequency decreases the amplitude increases as well as the depth increases. A similar but opposite behavior for phase fluctuation spectra is observed. As noted due to the presence of $\tilde{\gamma}$ the peak positions of the number and phase fluctuation spectra are not exactly at the Josephson frequency in the $\pi$-phase mode of the standard BJJ. This signifies that the peak frequency is modified by $\tilde{\gamma}$. The modification is a direct consequence of the frequency fluctuations in the energy levels with excitation-deexcitation in the system mode and is an important feature in the coherent behavior of the 1D dissipative BJJ.

Next we examine how the phase and number fluctuations change on increasing dissipation in the system in the zero-phase mode. In Figs. 6(a) and 6(b) we plot the number and phase fluctuation spectra as a function of detuning for several values of dissipation coefficient $\tilde{\gamma}$ for $N = 1000$. It is apparent that with an increase of $\tilde{\gamma}$ the two-peak structure reduces to one peak in each case indicating a transition from coherent to incoherent regime. The coherent regime implies the standard BJJ picture where the system oscillates between the two wells with a frequency close to the Josephson frequency, whereas for the incoherent regime the tunneling is prohibited.

We now study the effect of dissipation on number and phase fluctuation spectra in the $\pi$-phase mode Josephson oscillation regime. In Figs. 7(a) and 7(b) we plot the number and
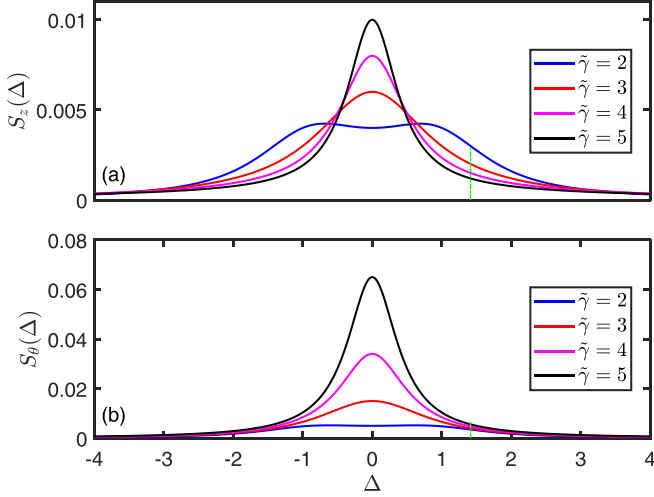
FIG. 7. Variations of $\mathcal{S}_z(\Delta)$ (a) and $\mathcal{S}_\theta(\Delta)$ (b) as a function of $\Delta$ for different values of $\tilde{\gamma}$ in the $\pi$-phase Josephson oscillation regime for $U/K = 0.001$, with $N = 1000$ and $k_B T/\hbar\Omega = 1/10$. The green dashed-dotted line indicates the Josephson frequency in the $\pi$-phase mode in the absence of dissipation.

phase fluctuation spectra as a function of detuning for several values of dissipation strength. The results are qualitatively similar to the earlier case. The difference, however, is that in the $\pi$-phase mode one reaches the incoherent regime for weak dissipation compared to the zero-phase mode for which one observes a transition from the coherent to incoherent regime for comparatively large values of $\tilde{\gamma}$.

Next we explore the fluctuation spectra for the weak and strong dissipative regime for the $\pi$-phase self-trapping mode. In Figs. 8(a) and 8(b) we plot the number and phase fluctuation spectra as a function of detuning for weak dissipation
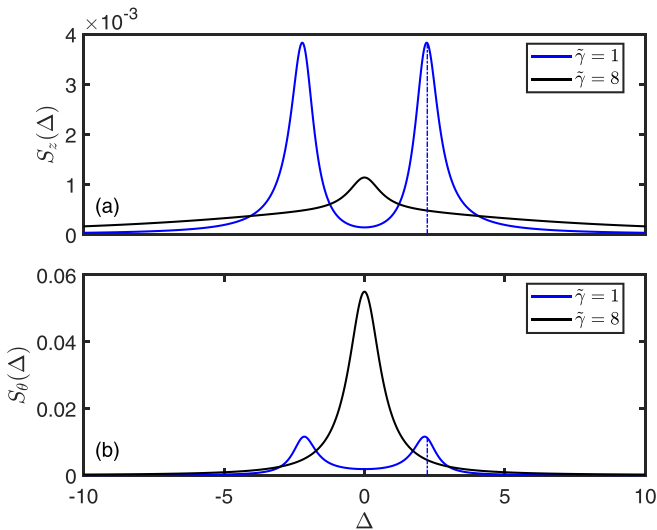


FIG. 8. Variations of $\mathcal{S}_z(\Delta)$ (a) and $\mathcal{S}_\theta(\Delta)$ (b) as a function of $\Delta$ for $\tilde{\gamma} = 1$ (solid blue line) and $\tilde{\gamma} = 8$ (solid black line) in the $\pi$-phase mode self-trapping regime for $U/K = 0.003$, with $N = 1000$ and $k_B T/\hbar\Omega = 1/10$. The blue dashed-dotted line indicates the self-trapping frequency in the $\pi$-phase mode in the absence of dissipation.

($\tilde{\gamma} = 1$) and strong dissipation ($\tilde{\gamma} = 8$). In the $\pi$-phase self-trapping regime, we choose the value of on-site interaction energy $U/K > 0.002$ such that the many-body interaction parameter $\Lambda_0$ becomes greater than unity. We observe that for weak dissipation ($\tilde{\gamma} = 1$ the solid blue line) the number and phase fluctuation spectra show the two peaks implying the coherent behavior where the peak amplitudes of the fluctuation spectra are at the $\pi$-phase mode self-trapping frequency denoted by the dashed-dotted blue line in Fig. 8. This picture qualitatively describes the coherent behavior of the 1D dissipative BJJ in the range of small dissipation where both number and phase of the atoms in the wells oscillate with nonzero average value. For strong dissipation ($\tilde{\gamma} = 8$), we observe that a single peak appears at $\Delta = 0$ in the fluctuation spectra. However, the amplitude of the phase fluctuation spectra is always greater than that for the number fluctuation spectra.

## VI. CONCLUSION

In this paper we have considered the dissipative BJJ within a two-mode Hamiltonian description. The key point of the study is the nonlinear coupling between the system and the bath modes such that the coherent excitation-deexcitation of the system modes brings out frequency fluctuation, which later gives rise to decoherence in the system. We have derived the associated quantum Langevin equations for the relative phase and population imbalance for the two BJJ modes. Quantum fluctuations around the three steady states of the dynamics, zero-phase mode, $\pi$-phase mode, and $\pi$-phase self-trapping mode, have been analyzed for several ranges of interaction parameter $\Lambda_0$ (measured in terms of the ratio of the strength of on-site interaction and tunneling), temperature $T$, and system-assisted dissipation coefficient $\tilde{\gamma}$, to explore the coherence factor, phase diffusion coefficient, and fluctuation spectra for population imbalance and phase difference. Our observations on the variation of coherence factor as well as the phase transition-like behavior of the phase diffusion coefficient between Josephson oscillation and MQST regime as a function of interaction parameter $\Lambda_0$ and the splitting and frequency shift of the Josephson frequency in the spectra are, we believe, amenable to experimental investigation within the scope of bath engineering. As the dissipation here is system-assisted it may be worthwhile to consider excitation-deexcitation of the chosen BJJ modes driven by an external field within the broadband of the frequency response of the bath. The on-site interaction-induced splitting and the shift of the Josephson frequency for the three modes are directly measurable quantities from the measurement of fluctuation spectra.

## APPENDIX A: DETAILED DERIVATION OF HEISENBERG EQUATIONS OF MOTION FOR THE SYSTEM AND BATH OPERATORS

Formal integration of Eqs. (8) and (9) yields

$$\hat{b}_{Lk}(t) = \hat{b}_{Lk}(t_0)e^{-i\omega_k(t-t_0)}$$
$$- ig_k \int_{t_0}^{t} \hat{a}_L^\dagger(t')\hat{a}_L(t')e^{-i\omega_k(t-t')} dt', \quad \text{(A1)}$$

$$\hat{b}_{Rk}(t) = \hat{b}_{Rk}(t_0)e^{-i\omega_k(t-t_0)}$$

$$-ig_k \int_{t_0}^t \hat{a}_R^\dagger(t')\hat{a}_R(t')e^{-i\omega_k(t-t')}\,dt', \quad \text{(A2)}$$

where the first term is the free evolution of bath operators, whereas the second term arises due to the interaction with the system. Inserting Eqs. (A1) and (A2) in Eqs. (6) and (7) we get

$$\dot{a}_L = -\frac{iE}{\hbar}\hat{a}_L + \frac{iK}{\hbar}\hat{a}_R - \frac{iU_+}{\hbar}\hat{a}_L^\dagger\hat{a}_L\hat{a}_L$$

$$- i\sum_k g_k \hat{b}_{Lk}(t_0)e^{-i\omega_k(t-t_0)}\hat{a}_L$$

$$- \sum_k g_k^2 \int_{t_0}^t \hat{a}_L^\dagger(t')\hat{a}_L(t')\hat{a}_L(t)e^{-i\omega_k(t-t')}\,dt', \quad \text{(A3)}$$

$$\dot{a}_R = -\frac{iE}{\hbar}\hat{a}_R + \frac{iK}{\hbar}\hat{a}_L - \frac{iU_-}{\hbar}\hat{a}_R^\dagger\hat{a}_R\hat{a}_R$$

$$- i\sum_k g_k \hat{b}_{Rk}(t_0)e^{-i\omega_k(t-t_0)}\hat{a}_R$$

$$- \sum_k g_k^2 \int_{t_0}^t \hat{a}_R^\dagger(t')\hat{a}_R(t')\hat{a}_R(t)e^{-i\omega_k(t-t')}\,dt'. \quad \text{(A4)}$$

Changing the integration variable from $t'$ to $\tau = t - t'$ in Eq. (A3), we may write the last term in Eq. (A3) as $\sum_k g_k^2 \int_0^{t-t_0} \hat{a}_L^\dagger(t-\tau)\hat{a}_L(t-\tau)\hat{a}_L(t-\tau)e^{-i\omega_k\tau}d\tau$, where we have approximated $\hat{a}_L(t) = \hat{a}_L(t-\tau)$ for the last annihilation operator, since the interference time $\tau_c$ of $\sum_k g_k^2 e^{-i\omega_k\tau}$ is much smaller than the time over which the amplitude and the phase modulation of $a_L(t)$ take place. Thus for times $t - t_0 > \tau_c$, $\tau_c \to 0$, the summation acts as a delta function so that we may write the integral approximately as $\hat{a}_L^\dagger\hat{a}_L\hat{a}_L \int_0^\infty d\tau \sum_k g_k^2 e^{-i(E/\hbar-\omega_k)\tau}$. Assuming that the bath modes are closely spaced in frequency we replace the summation over $k$ by an integral over $\omega$, i.e., $\sum_k \to \int d\omega \Theta(\omega)$, where $\Theta(\omega)$ is the density of states. This density and $g(\omega)$ are proportional to the powers of $\omega$ and vary very little in the frequency interval $\tau^{-1}$ over $\omega$. This leads us to the following two equations for the reduced dynamics [the same procedure is followed for Eq. (A4)]:

$$\dot{a}_L = -\frac{iE}{\hbar}\hat{a}_L + \frac{iK}{\hbar}\hat{a}_R - \frac{iU_+}{\hbar}\hat{a}_L^\dagger\hat{a}_L\hat{a}_L - \frac{\gamma}{2}\hat{a}_L^\dagger\hat{a}_L\hat{a}_L + \hat{f}_L(t)\hat{a}_L,$$
$$\text{(A5)}$$

$$\dot{a}_R = -\frac{iE}{\hbar}\hat{a}_R + \frac{iK}{\hbar}\hat{a}_L - \frac{iU_-}{\hbar}\hat{a}_R^\dagger\hat{a}_R\hat{a}_R - \frac{\gamma}{2}\hat{a}_R^\dagger\hat{a}_R\hat{a}_R + \hat{f}_R(t)\hat{a}_R,$$
$$\text{(A6)}$$

where $\gamma = 2\pi g^2(\Omega)\Theta(\Omega)$ represents the dissipation of the modes and $\Omega = E/\hbar$. $\Theta(\Omega)$ is the density of the bath modes. The terms $\hat{f}_L(t) = -i\sum_k g_k(t_0)\hat{b}_{Lk}(t_0)e^{-i\omega_k(t-t_0)}$ and $\hat{f}_R(t) = -i\sum_k g_k(t_0)\hat{b}_{Rk}(t_0)e^{-i\omega_k(t-t_0)}$ refer to quantum noise due to the heat baths for the $L$ and $R$ modes.

## APPENDIX B: QUANTUM AND THERMAL PROPERTIES OF NOISE

The noise properties of the operator $\hat{F}_{L,R}$ and $\hat{F}_{L,R}^\dagger$ in Eqs. (12) and (13) can be derived using a suitable canonical thermal distribution of the bath operators at $t_0 = 0$. To this end we define the quantum statistical average of any reservoir operator $\hat{O}$:

$$\langle\hat{O}\rangle_{\text{qs}} = \frac{\text{Tr}[\hat{O}\exp(-\hat{H}_R/k_BT)]}{\text{Tr}[\exp(-\hat{H}_R/k_BT)]}, \quad \text{(B1)}$$

where $\hat{H}_R = \sum_j \hbar\omega_j\hat{n}_j$ at $t_0 = 0$ and $\hat{n}_j$ denotes the number operator in $j$th bath mode. Based on the above considerations the noise properties of the operator may be calculated using the canonical distribution of Eqs. (12) and (13). This immediately gives $\langle\hat{F}_{L,R}(t)\rangle_{\text{qs}} = 0$ and $\langle\hat{F}_{L,R}^\dagger(t)\rangle_{\text{qs}} = 0$ and $\langle\hat{F}_{L,R}^\dagger(t)\hat{F}_{L,R}(t')\rangle_{\text{qs}} = \gamma\bar{n}_{L,R}(\Omega)\delta(t-t')$ and $\langle\hat{F}_{L,R}(t)\hat{F}_{L,R}^\dagger(t')\rangle_{\text{qs}} = \gamma[\bar{n}_{L,R}(\Omega)+1]\delta(t-t')$. The fluctuation-dissipation relation gives

$$\langle\hat{F}_{L,R}^\dagger(t)\hat{F}_{L,R}(t') + \hat{F}_{L,R}(t)\hat{F}_{L,R}^\dagger(t')\rangle_{\text{qs}}$$

$$= \gamma[2\bar{n}_{L,R}(\Omega)+1]\delta(t-t')$$

$$= \gamma\coth(\hbar\Omega/2k_BT)\delta(t-t'), \quad \text{(B2)}$$

where the contangent hyperbolic factor in Eq. (B2) can be identified with the Bose-Einstein distribution

$$\bar{n}_{L,R}(\Omega) = \frac{1}{e^{\hbar\Omega/k_BT}-1} \quad \text{(B3)}$$

using the relation $2\bar{n}_{L,R}(\Omega)+1 = \coth(\hbar\Omega/2k_BT)$ and the plus one factor is responsible for the vacuum fluctuation, which is always present on the quantum scale even at absolute zero temperature.

Now to realize $\xi_{L,R}(t)$ as an effective $c$-number noise, we introduce the ansatz that $\mu_{Lk,Rk}(0)$ and $\mu_{Lk,Rk}^*(0)$ are distributed according to the Wigner thermal canonical distribution of the Gaussian form [78,92] as follows:

$$W_{Lk,Rk}[\mu_{Lk,Rk}(0), \mu_{Lk,Rk}^*(0)]$$

$$= N_{BL,BR}\exp\left[-\frac{|\mu_{Lk,Rk}(0)|^2}{2\coth\left(\frac{\hbar\Omega}{2k_BT}\right)}\right]. \quad \text{(B4)}$$

Here $N_{BL,BR}$ is the normalization constant for $L$ and $R$ wells and $\coth(\frac{\hbar\Omega}{2k_BT})$ is the width of the distribution. For any arbitrary quantum mechanical mean value of the bath operator $\langle\hat{B}_{Lk,Rk}\rangle$ which is a function of $\mu_{Lk,Rk}(0)$, $\mu_{Lk,Rk}^*(0)$, its statistical average can then be calculated as

$$\langle\langle\hat{B}_{Lk,Rk}\rangle\rangle_s = \int \langle\hat{B}_{Lk,Rk}\rangle W_{Lk,Rk}[\mu_{Lk,Rk}(0),$$

$$\times \mu_{Lk,Rk}^*(0)]\,d\mu_{Lk,Rk}(0)\,d\mu_{Lk,Rk}^*(0). \quad \text{(B5)}$$

Using the ansatz (B4) and the definition of statistical average of Eq. (B5), one can show that the $c$-number noise satisfies the following relations:

$$\langle\xi_{L,R}(t)\rangle_s = 0,$$
$$\langle\xi_{L,R}^*(t)\rangle_s = 0, \quad \text{(B6)}$$

and

$$\langle\xi_{L,R}^*(t)\xi_{L,R}(t')\rangle_s = \gamma\coth(\hbar\Omega/2k_BT)\delta(t-t'),$$

$$\langle\xi_{L,R}(t)\xi_{L,R}^*(t')\rangle_s = \gamma\coth(\hbar\Omega/2k_BT)\delta(t-t'). \quad \text{(B7)}$$

Equations (B6) and (B7) imply that the $c$-number noise $\xi_{L,R}(t)$ is characterized by zero mean and follow the fluctuation-

dissipation relation. The use of the Wigner canonical thermal distribution function [92] is mainly motivated by the fact that once the averaging procedure as carried out in two steps (first, quantum mechanical average over the operators for the bath variables; second, statistical averaging with Wigner canonical distribution of the *c*-numbers) is fixed, one arrives at the Langevin equation in *c*-numbers directly. By using the *c*-number formalism, we may thus bypass the operator-ordering prescription for the derivation of noise properties. Once the noise properties are derived it is easy to formulate the Fokker-Planck equation for *c*-number variables and to calculate the correlation functions and fluctuation spectra. The *c*-number noise $\xi_{L,R}(t)$ as characterized by Eqs. (B6) and (B7) is classical looking in form but essentially quantum mechanical in nature [95].

## APPENDIX C: DETAILED DERIVATION OF EQS. (16) AND (17) FROM EQS. (14) AND (15)

We return to the classical field equations for the two wells as given by Eqs. (14) and (15). The *c*-number amplitudes may be written as $\alpha_L = \sqrt{N_L}e^{i\theta_L}$, and $\alpha_R = \sqrt{N_R}e^{i\theta_R}$, which give

$$\dot{\alpha_L} = \frac{e^{i\theta_L}}{2\sqrt{N_L}} \frac{\partial N_L}{\partial t} + i\sqrt{N_L}e^{i\theta_L} \frac{\partial \theta_L}{\partial t},$$

$$\dot{\alpha_R} = \frac{e^{i\theta_R}}{2\sqrt{N_R}} \frac{\partial N_R}{\partial t} + i\sqrt{N_R}e^{i\theta_R} \frac{\partial \theta_R}{\partial t}.$$

From the above two equations and Eqs. (14) and (15), we find

$$\frac{1}{2\sqrt{N_L}} \frac{\partial N_L}{\partial t} + i\sqrt{N_L} \frac{\partial \theta_L}{\partial t} = \frac{iK}{\hbar} \sqrt{N_R}e^{i(\theta_R-\theta_L)} - \frac{iU_+}{\hbar} N_L\sqrt{N_L} - \frac{\gamma}{2}N_L\sqrt{N_L} + \left(\xi_L^{\text{real}} + i\xi_L^{\text{im}}\right)\sqrt{N_L}, \tag{C1}$$

$$\frac{1}{2\sqrt{N_R}} \frac{\partial N_R}{\partial t} + i\sqrt{N_R} \frac{\partial \theta_R}{\partial t} = \frac{iK}{\hbar} \sqrt{N_L}e^{-i(\theta_R-\theta_L)} - \frac{iU_-}{\hbar} N_R\sqrt{N_R} - \frac{\gamma}{2}N_R\sqrt{N_R} + \left(\xi_R^{\text{real}} + i\xi_R^{\text{im}}\right)\sqrt{N_R}. \tag{C2}$$

Now equating the real parts of Eqs. (C1) and (C2) we obtain

$$\frac{\partial N_L}{\partial t} = -\frac{2K}{\hbar} \sqrt{N_L N_R} \sin(\theta_R - \theta_L) - \gamma N_L^2 + 2\xi_L^{\text{real}}N_L, \tag{C3}$$

$$\frac{\partial N_R}{\partial t} = \frac{2K}{\hbar} \sqrt{N_L N_R} \sin(\theta_R - \theta_L) - \gamma N_R^2 + 2\xi_R^{\text{real}}N_R. \tag{C4}$$

From the imaginary parts of Eqs. (C1) and (C2) we find

$$\hbar\frac{\partial \theta_L}{\partial t} = K\sqrt{\frac{N_R}{N_L}} \cos(\theta_R - \theta_L) - U_+N_L + \hbar\xi_L^{\text{im}}, \tag{C5}$$

$$\hbar\frac{\partial \theta_R}{\partial t} = K\sqrt{\frac{N_L}{N_R}} \cos(\theta_R - \theta_L) - U_-N_R + \hbar\xi_R^{\text{im}}. \tag{C6}$$

Now, subtraction of Eq. (C3) from (C4) and division by the total number $N = N_L + N_R$ results in

$$\dot{z}(t) = -\frac{4K}{\hbar} \frac{\sqrt{N_L N_R}}{(N_L + N_R)} \sin(\theta_R - \theta_L) - \gamma(N_L - N_R) + \frac{2\xi_L^{\text{real}}N_L}{N} - \frac{2\xi_R^{\text{real}}N_R}{N}.$$

Furthermore the substitution $\frac{2\sqrt{N_L N_R}}{(N_L + N_R)} = \sqrt{1 - z^2(t)}$ gives

$$\dot{z}(t) = -\frac{2K}{\hbar} \sqrt{1 - z^2(t)} \sin(\theta_R - \theta_L) - \gamma(N_L - N_R) + \frac{2\xi_L^{\text{real}}N_L}{N} - \frac{2\xi_R^{\text{real}}N_R}{N}.$$

As a result the equation for population imbalance becomes

$$\dot{z}(t) = -\frac{2K}{\hbar} \sqrt{1 - z^2(t)} \sin\theta(t) - \gamma N z(t) + \xi_z. \tag{C7}$$

Now on subtracting Eq. (C6) from (C5), we get

$$\hbar\left(\frac{\partial \theta_R}{\partial t} - \frac{\partial \theta_L}{\partial t}\right) = K\cos(\theta_R - \theta_L)\left[\sqrt{\frac{N_L}{N_R}} - \sqrt{\frac{N_R}{N_L}}\right] + U_+N_L - U_-N_R + \hbar\xi_R^{\text{im}} - \hbar\xi_L^{\text{im}}.$$

We make use of the relation $\frac{z}{\sqrt{1-z^2}} = \frac{N_L - N_R}{2\sqrt{N_L N_R}}$ to obtain

$$\dot{\theta}(t) = \frac{2K}{\hbar}\left[\frac{z(t)}{\sqrt{1 - z^2(t)}} \cos\theta + \frac{U_+N_L - U_-N_R}{2K}\right] + \xi_R^{\text{im}} - \xi_L^{\text{im}}. \tag{C8}$$

Finally by noting

$$\frac{U_+N_L - U_-N_R}{2K} = \frac{U_+ - U_-}{4K}N + \frac{NU}{2K}z(t)$$

Eq. (C8) becomes

$$\dot{\theta}(t) = \frac{2K}{\hbar} \left[ \frac{z(t)}{\sqrt{1 - z^2(t)}} \cos\theta(t) + \frac{U_+ - U_-}{4K} N + \frac{NU}{2K} z(t) \right] + \xi_\theta$$

For a symmetric DW, we write $U_+ = U_-$. As a result, the above equation becomes

$$\dot{\theta}(t) = \frac{2K}{\hbar} \left[ \frac{z(t)}{\sqrt{1 - z^2(t)}} \cos\theta(t) + \frac{NU}{2K} z(t) \right] + \xi_\theta. \tag{C9}$$

[1] U. Weiss, *Quantum Dissipative Systems* (World Scientific, Singapore, 2008).

[2] H. P. Breuer and F. Petruccione, *The Theory of Open Quantum Systems* (Oxford University Press, Oxford, 2007).

[3] A. O. Caldeira and A. J. Leggett, Phys. Rev. Lett. **46**, 211 (1981).

[4] G. W. Ford, J. T. Lewis, and R. F. O'Connell, Phys. Rev. A **37**, 4419 (1988).

[5] A. Schmid, Phys. Rev. Lett. **51**, 1506 (1983).

[6] S. A. Bulgadaev, Pis'ma Zh. Eksp. Teor. Fiz. **39**, 264 (1984) [JETP Lett. **39**, 315 (1984)].

[7] E. G. Dalla Torre, E. Demler, T. Giamarchi, and E. Altman, Nat. Phys. **6**, 806 (2010).

[8] S. Diehl, A. Micheli, A. Kantian, B. Kraus, H. P. Büchler, and P. Zoller, Nat. Phys. **4**, 878 (2008).

[9] J. T. Barreiro, M. Müller, P. Schindler, D. Nigg, T. Monz, M. Chwalla, M. Hennrich, C. F. Roos, P. Zoller, and R. Blatt, Nature (London) **470**, 486 (2011).

[10] M. Müller, S. Diehl, G. Pupillo, and P. Zoller, Adv. At. Mol. Opt. Phys. **61**, 1 (2012).

[11] D. Dalidovich and M. P. Kennett, Phys. Rev. A **79**, 053611 (2009).

[12] L. M. Sieberer, S. D. Huber, E. Altman, and S. Diehl, Phys. Rev. Lett. **110**, 195301 (2013).

[13] T. Graß, Phys. Rev. A **99**, 043607 (2019).

[14] A. Le Boité, G. Orso, and C. Ciuti, Phys. Rev. Lett. **110**, 233601 (2013).

[15] M. P. Kennett and D. Dalidovich, Phys. Rev. A **84**, 033620 (2011).

[16] A. K. Saha and R. Dubessy, Phys. Rev. A **104**, 023316 (2021).

[17] S. Diehl, A. Tomadin, A. Micheli, R. Fazio, and P. Zoller, Phys. Rev. Lett. **105**, 015702 (2010).

[18] T. E. Lee, H. Häffner, and M. C. Cross, Phys. Rev. A **84**, 031402(R) (2011).

[19] M. Marcuzzi, E. Levi, S. Diehl, J. P. Garrahan, and I. Lesanovsky, Phys. Rev. Lett. **113**, 210401 (2014).

[20] S. Ray, S. Sinha, and K. Sengupta, Phys. Rev. A **93**, 033627 (2016).

[21] I. Zapata, F. Sols, and A. J. Leggett, Phys. Rev. A **57**, R28(R) (1998).

[22] S. Ji, T. Schweigler, M. Tajik, F. Cataldini, J. Sabino, F. S. Møller, S. Erne, and J. Schmiedmayer, Phys. Rev. Lett. **129**, 080402 (2022).

[23] J. Polo, V. Ahufinger, F. W. J. Hekking, and A. Minguzzi, Phys. Rev. Lett. **121**, 090404 (2018).

[24] F. Binanti, K. Furutani, and L. Salasnich, Phys. Rev. A **103**, 063309 (2021).

[25] A. Kampf and G. Schön, Physica C **153–155**, 675 (1988).

[26] Y. M. Bidasyuk, M. Weyrauch, M. Momme, and O. O. Prikhodko, J. Phys. B: At. Mol. Opt. Phys. **51**, 205301 (2018).

[27] G. Mazzarella, L. Salasnich, and F. Toigo, J. Phys. B: At. Mol. Opt. Phys. **45**, 185301 (2012).

[28] S. Sinha and S. Sinha, Phys. Rev. E **100**, 032115 (2019).

[29] R. Gati, B. Hemmerling, J. Fölling, M. Albiez, and M. K. Oberthaler, Phys. Rev. Lett. **96**, 130404 (2006).

[30] M. Lewenstein and L. You, Phys. Rev. Lett. **77**, 3489 (1996).

[31] J. Javanainen and M. Wilkens, Phys. Rev. Lett. **78**, 4675 (1997).

[32] Y. Khodorkovsky, G. Kurizki, and A. Vardi, Phys. Rev. Lett. **100**, 220403 (2008).

[33] E. Boukobza, M. Chuchem, D. Cohen, and A. Vardi, Phys. Rev. Lett. **102**, 180403 (2009).

[34] R. Gommers, V. Lebedev, M. Brown, and F. Renzoni, Phys. Rev. Lett. **100**, 040603 (2008).

[35] M. Schiavoni, L. Sanchez-Palencia, F. Renzoni, and G. Grynberg, Phys. Rev. Lett. **90**, 094101 (2003).

[36] G. Tayebirad, A. Zenesini, D. Ciampini, R. Mannella, O. Morsch, E. Arimondo, N. Lörch, and S. Wimberger, Phys. Rev. A **82**, 013633 (2010).

[37] A. Yedjour, H. Benmahdjoub, and A. Boudjemâa, Phys. Scr. **97**, 025401 (2022).

[38] L. Sanchez-Palencia, Phys. Rev. E **70**, 011102 (2004).

[39] P. Sjölund, S. J. H. Petra, C. M. Dion, S. Jonsell, M. Nylén, L. Sanchez-Palencia, and A. Kastberg, Phys. Rev. Lett. **96**, 190602 (2006).

[40] P. Sjölund, S. J. H. Petra, C. M. Dion, H. Hagman, S. Jonsellb, and A. Kastberg, Eur. Phys. J. D **44**, 381 (2007).

[41] A. Vardi and J. R. Anglin, Phys. Rev. Lett. **86**, 568 (2001).

[42] J. R. Anglin and A. Vardi, Phys. Rev. A **64**, 013605 (2001).

[43] Y. Castin and J. Dalibard, Phys. Rev. A **55**, 4330 (1997).

[44] E. M. Wright, D. F. Walls, and J. C. Garrison, Phys. Rev. Lett. **77**, 2158 (1996).

[45] M. Greiner, O. Mandel, T. W. Hänsch, and I. Bloch, Nature (London) **419**, 51 (2002).

[46] G.-B. Jo, Y. Shin, S. Will, T. A. Pasquini, M. Saba, W. Ketterle, D. E. Pritchard, M. Vengalattore, and M. Prentiss, Phys. Rev. Lett. **98**, 030407 (2007).

[47] A. Widera, S. Trotzky, P. Cheinet, S. Fölling, F. Gerbier, I. Bloch, V. Gritsev, M. D. Lukin, and E. Demler, Phys. Rev. Lett. **100**, 140401 (2008).

[48] R. Labouvie, B. Santra, S. Heun, and H. Ott, Phys. Rev. Lett. **116**, 235302 (2016).

[49] H. Krauter, C. A. Muschik, K. Jensen, W. Wasilewski, J. M. Petersen, J. Ignacio Cirac, and E. S. Polzik, Phys. Rev. Lett. **107**, 080503 (2011).

[50] A. W. Laskar, P. Adhikary, S. Mondal, P. Katiyar, S. Vinjanampathy, and S. Ghosh, Phys. Rev. Lett. **125**, 013601 (2020).

[51] K. W. Murch, U. Vool, D. Zhou, S. J. Weber, S. M. Girvin, and I. Siddiqi, Phys. Rev. Lett. **109**, 183602 (2012).

[52] J. F. Mennemann, I. E. Mazets, M. Pigneur, H. P. Stimming, N. J. Mauser, J. Schmiedmayer, and S. Erne, Phys. Rev. Res. **3**, 023197 (2021).

[53] Y. D. van Nieuwkerk, J. Schmiedmayer, and F. H. L. Essler, SciPost Phys. **10**, 090 (2021).

[54] K. Xhani and N. P. Proukakis, Phys. Rev. Res. **4**, 033205 (2022).

[55] K Xhani, L. Galantucci, C. F. Barenghi, G. Roati, A. Trombettoni, and N. P. Proukakis, New J. Phys. **22**, 123006 (2020).

[56] Th. Anker, M. Albiez, R. Gati, S. Hunsmann, B. Eiermann, A. Trombettoni, and M. K. Oberthaler, Phys. Rev. Lett. **94**, 020403 (2005).

[57] L. J. LeBlanc, A. B. Bardon, J. McKeever, M. H. T. Extavour, D. Jervis, J. H. Thywissen, F. Piazza, and A. Smerzi, Phys. Rev. Lett. **106**, 025302 (2011).

[58] M. Abad, M. Guilleumas, R. Mayol, F. Piazza, D. M. Jezek, and A. Smerzi, Europhys. Lett. **109**, 40005 (2015).

[59] J. Polo, R. Dubessy, P. Pedri, H. Perrin, and A. Minguzzi, Phys. Rev. Lett. **123**, 195301 (2019).

[60] A. Griffin, S. Nazarenko, and D. Proment, J. Phys. A: Math. Theor. **53**, 175701 (2020).

[61] V. P. Singh, N. Luick, L. Sobirey, and L. Mathey, Phys. Rev. Res. **2**, 033298 (2020).

[62] Y. M. Bidasyuk, O. O. Prikhodko, and M. Weyrauch, Phys. Rev. A **94**, 033603 (2016).

[63] S. Martínez-Garaot, G. Pettini, and M. Modugno, Phys. Rev. A **98**, 043624 (2018).

[64] A. Burchianti, C. Fort, and M. Modugno, Phys. Rev. A **95**, 023627 (2017).

[65] D. V. Tsarev, D. V. Ansimov, S. A. Podoshvedov, and A. P. Alodjants, Laser Phys. Lett. **19**, 125202 (2022).

[66] A. Tameshtit and J. E. Sipe, Phys. Rev. A **47**, 1697 (1993).

[67] G. Gangopadhyay, M S Kumar, and S. Dattagupta, J. Phys. A: Math. Gen. **34**, 5485 (2001).

[68] J. Shao, M.-L. Ge, and H. Cheng, Phys. Rev. E **53**, 1243 (1996).

[69] Y. Tanimura and T. Steffen, J. Phys. Soc. Jpn. **69**, 4095 (2000).

[70] Y. Ming, H.-M. Li, and Z.-J. Ding, Phys. Rev. E **93**, 032127 (2016).

[71] L. N. Wu and A. Eckardt, SciPost Phys. **13**, 059 (2022).

[72] F. Damanet, E. Mascarenhas, D. Pekker, and A. J. Daley, New J. Phys. **21**, 115001 (2019).

[73] J. F. Poyatos, J. I. Cirac, and P. Zoller, Phys. Rev. Lett. **77**, 4728 (1996).

[74] J. Piilo and S. Maniscalco, Phys. Rev. A **74**, 032303 (2006).

[75] D. Bacon, A. M. Childs, I. L. Chuang, J. Kempe, D. W. Leung, and X. Zhou, Phys. Rev. A **64**, 062302 (2001).

[76] S. Fedortchenko, A. Keller, T. Coudreau, and P. Milman, Phys. Rev. A **90**, 042103 (2014).

[77] S. L. Vuglar, D. V. Zhdanov, R. Cabrera, T. Seideman, C. Jarzynski, and D. I. Bondar, Phys. Rev. Lett. **120**, 230404 (2018).

[78] M. Hillery, R. O'Connell, M. Scully, and E. Wigner, Phys. Rep. **106**, 121 (1984).

[79] L. Pitaevskii and S. Stringari, Phys. Rev. Lett. **87**, 180402 (2001).

[80] A. K. Saha, K. Adhikary, S. Mal, K. R. Dastidar, and B. Deb, J. Phys. B: At. Mol. Opt. Phys. **52**, 155301 (2019).

[81] A. K. Saha, D. S. Ray, and B. Deb, J. Phys. B: At. Mol. Opt. Phys. **53**, 135301 (2020).

[82] S. Raghavan, A. Smerzi, S. Fantoni, and S. R. Shenoy, Phys. Rev. A **59**, 620 (1999).

[83] G. Spagnolli, G. Semeghini, L. Masi, G. Ferioli, A. Trenkwalder, S. Coop, M. Landini, L. Pezzè, G. Modugno, M. Inguscio, A. Smerzi, and M. Fattori, Phys. Rev. Lett. **118**, 230403 (2017).

[84] M. Albiez, R. Gati, J. Fölling, S. Hunsmann, M. Cristiani, and M. K. Oberthaler, Phys. Rev. Lett. **95**, 010402 (2005).

[85] M. Pigneur and J. Schmiedmayer, Phys. Rev. A **98**, 063632 (2018).

[86] M. Pigneur, T. Berrada, M. Bonneau, T. Schumm, E. Demler, and J. Schmiedmayer, Phys. Rev. Lett. **120**, 173601 (2018).

[87] D. Stefanatos and E. Paspalakis, Phys. Lett. A **383**, 2370 (2019).

[88] W. Louisell, *Quantum Statistical Properties of Radiation* (Wiley, New York, 1973).

[89] H. Carmichael, *Statistical Methods in Quantum Optics 1: Master Equations and Fokker-Planck Equations, Physics and Astronomy Online Library* (Springer, Berlin, 1999).

[90] G. S. Agarwal, *Quantum Optics* (Cambridge University Press, Cambridge, 2013).

[91] D. Barik, D. Banerjee, and D. S. Ray, *Quantum Brownian Motion in C-numbers: Theory and Applications* (Nova Science, New York, 2005).

[92] A. Ghosh, S. S. Sinha, and D. S. Ray, Phys. Rev. E **86**, 011122 (2012).

[93] I. Marino, S. Raghavan, S. Fantoni, S. R. Shenoy, and A. Smerzi, Phys. Rev. A **60**, 487 (1999).

[94] T. Zibold, E. Nicklas, C. Gross, and M. K. Oberthaler, Phys. Rev. Lett. **105**, 204101 (2010).

[95] G. Ingold, A. Buchleitner, and K. Hornberger, *Coherent Evolution in Noisy Environments* (Springer, Berlin, 2002).